

A Variable Switching Frequency Approach to Reduce the Output Current Ripple of Single-Phase PWM Inverters

Pekik Argo Dahono¹, Masramdhani Saputra², and Arwindra Rizqiawan¹

¹School of Electrical Engineering and Informatics, Institut Teknologi Bandung

²Malang State Polytechnic
pekik@konversi.ee.itb.ac.id

Abstract: A new variable switching frequency is proposed to reduce the output current ripple of single-phase PWM inverters. This proposed method will keep the peak-to-peak output current ripple constant, instead of varying as the function of current angle in the conventional constant switching frequency operation. By keeping the constant peak-to-peak current ripple, the output current ripple can be reduced without sacrificing the efficiency. Analytical expression for the optimum switching frequency variation is derived. Experiment results are included to show and verify the effectiveness of the proposed method.

Keywords: inverter, current ripple, PWM

1. Introduction

Along with the development of power semiconductor devices and the associated controller, more widespread use of power electronics can be seen in the last decades. One type of power converter that is widely used is the inverter. For small and medium power applications, a single-phase inverter is commonly used [1]. In the recent years, a single-phase full-bridge inverter has also been proposed as a basic building block for a large power and high-voltage applications.

There are many PWM techniques have been developed to control the output voltage and frequency of single-phase inverters. Carrier-based PWM technique is the most popular because the implementation is simpler. In this technique, the ON-OFF signals for the inverter switching devices are obtained by comparing a sinusoidal reference signal to a high-frequency triangular carrier signal. To reduce the output current ripple, the carrier or switching frequency must be increased. By increasing the switching frequency, however, the inverter switching losses are also increased. Until now, soft switching techniques are not commonly used in high power applications because of the increased voltage or current stresses on the inverter switching devices. Variable switching frequency techniques to reduce the output current ripple of three-phase inverter have also been proposed [2]-[5]. Other works in the field of variable-band on hysteresis current control to achieve nearly constant switching frequency are also have been proposed [6]-[10], but most of the proposed methods require more complex control thus sacrifice the well-known advantage of hysteresis current controller, which is simplicity. Until now, however, no works have shown what is the optimum switching frequency variation that is useful for single-phase full-bridge inverters.

In this paper, a new approach to reduce the output current ripple of single phase PWM inverter without sacrificing the inverter efficiency is proposed. At first, the optimum switching frequency variation that results in minimum output current ripple is determined. Simulated and measured results are included to verify and show the effectiveness of the proposed concept.

2. Single-Phase PWM Inverter

Figure 1 shows the scheme of inverter that is used in this study. The load is represented as a series connection of a resistance R , and inductance L , and a sinusoidal emf e . The dc voltage source E_d is assumed as a constant and free of ripple. It should be noted that this inverter scheme can also be used to represent a single-phase PWM rectifier, by reversing the power flow direction.

Received: November 21st, 2016. Accepted: March 11st, 2017

DOI: 10.15676/ijeei.2017.9.1.6

In this paper, it is assumed that the ON-OFF signals for the switching devices are obtained by using a carrier based PWM technique. In this technique, two identical sinusoidal reference signals that opposite in phase are compared to a high-frequency triangular signal as shown in Figure. 2, this is well-known as unipolar PWM technique. Comparison results between the first sinusoidal signal and carrier signal are used to control switching devices on the left leg (S1 and S2). On the other hand, comparison results between the second sinusoidal signal and carrier signal will be described in the next sections, it is assumed that the inverter switching devices are ideal switches.

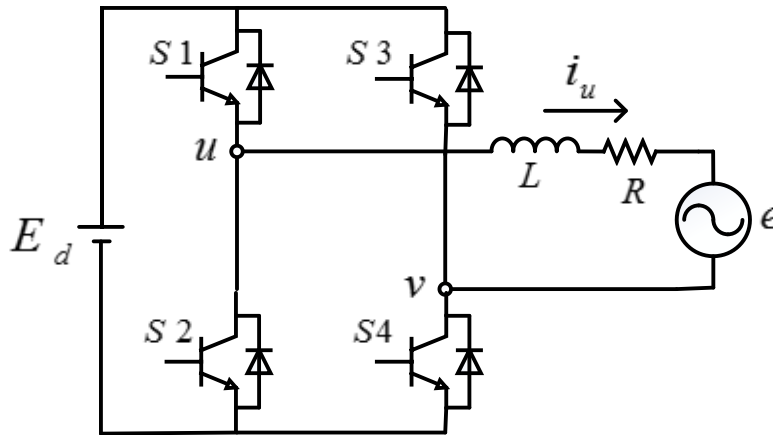


Figure 1. Single-phase full-bridge PWM inverter.

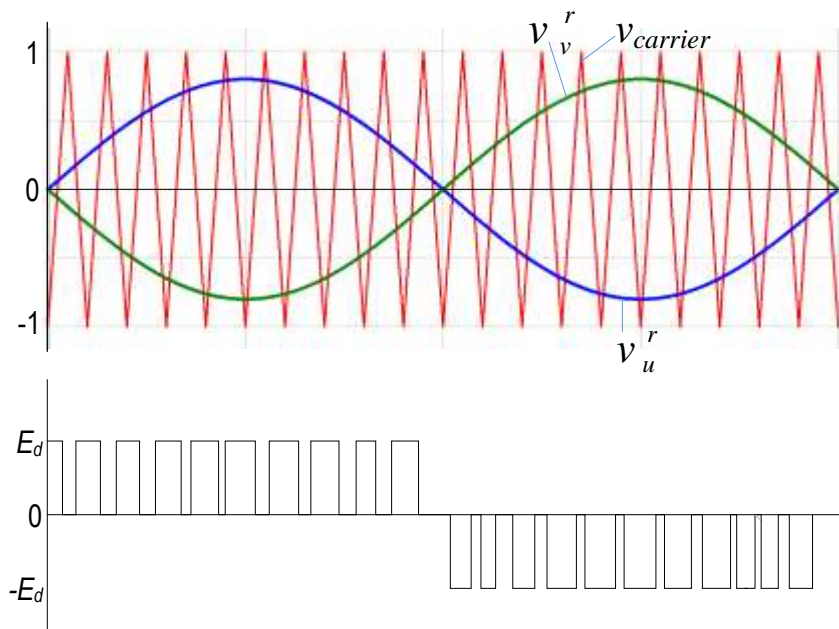


Figure 2. PWM signal generation (upper) and inverter output voltage (lower).

3. Output Current Ripple Analysis

In order to reduce the output current ripple, the switching frequency is usually much higher than the fundamental output frequency. Under this condition, the reference signals over one carrier period can be assumed as constants as shown in Figure. 3(a). Based on Figure. 3(a), the

output voltage over one carrier period can be obtained as shown in Figure. 3(b). Figure. 3 is valid during positive half fundamental period of output voltage.

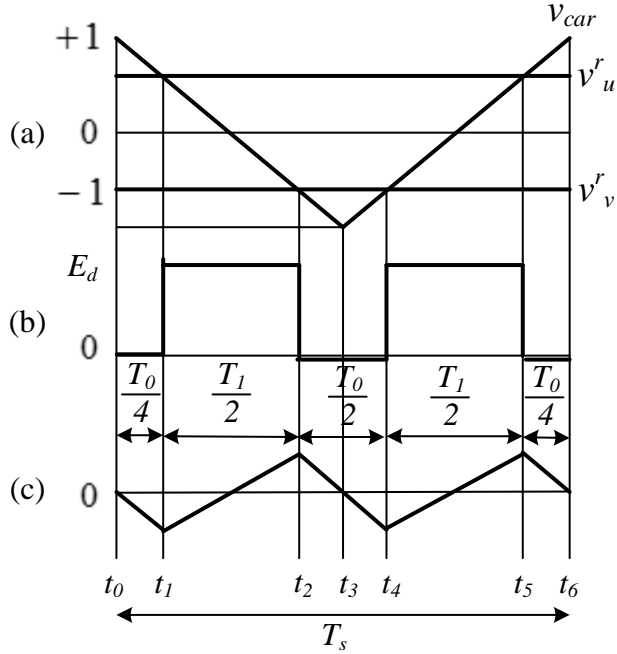


Figure. 3. Waveforms of the inverter over one carrier period. (a) Reference voltage, (b) Output voltage, (c) current ripple

The output voltage over one carrier period can be expressed as follow:

$$v_{uv} = \begin{cases} 0 & \text{for } t_0 < t \leq t_1 \\ E_d & \text{for } t_1 < t \leq t_2 \\ 0 & \text{for } t_2 < t \leq t_4 \\ E_d & \text{for } t_4 < t \leq t_5 \\ 0 & \text{for } t_5 < t \leq t_6 \end{cases} \quad (1)$$

Where v_{uv} is the output voltage of single-phase inverter, as in Figure. 1. Based on Figure. 3, the time intervals are:

$$\frac{T_0}{T_s} = 1 - v_u^r \quad (2)$$

$$\frac{T_1}{T_s} = v_u^r \quad (3)$$

Where v_u^r is the voltage reference signal, and its value is determined by

$$v_u^r = k \sin \theta \quad (4)$$

Where k is the modulation index, $T_s = 1/F_s$ is the carrier period, and θ is the angle of the reference signal at the moment of corresponding period of carrier signal.

Based on the scheme in Figure. 1, the voltage across the load is

$$v_{uv} = Ri_u + L \frac{di_u}{dt} + e \quad (5)$$

Where i_u is the output current.

If the voltage and current are separated into the average and ripple components, Eq. (2) can be rewritten as

$$\bar{v}_{uv} + \tilde{v}_{uv} = R(\bar{i}_u + \tilde{i}_u) + L \frac{d}{dt}(\bar{i}_u + \tilde{i}_u) + e \quad (6)$$

where bar and tilde over variables denote average and ripple components, respectively. Average and ripple components on the left hand side of Eq. (6) must be equal to average and ripple components on the right hand side and, therefore, the followings are obtained:

$$\bar{v}_{uv} = R\bar{i}_u + L \frac{d\bar{i}_u}{dt} + e \quad (7)$$

$$\tilde{v}_{uv} = v_{uv} - \bar{v}_{uv} = R\tilde{i}_u + L \frac{d\tilde{i}_u}{dt} \quad (8)$$

The average output voltage as a function of the reference signal can be written as

$$\bar{v}_{uv} = kE_d \sin \theta \quad (9)$$

When the switching frequency is high, the ripple voltage across the load resistance is usually small and can be neglected. Thus, Eq. (8) can be approximated by

$$\tilde{v}_{uv} = L \frac{d\tilde{i}_u}{dt} \quad (10)$$

Thus, the current ripple can be expressed as

$$\tilde{i}_u = \frac{1}{L} \int \tilde{v}_{uv} dt = \frac{1}{L} \int (v_{uv} - \bar{v}_{uv}) dt \quad (11)$$

Based on voltage expression in Eq. (1) and current ripple expression in Eq. (11), the current ripple waveform can be obtained as shown in Figure. 3(c). This current ripple can be expressed as

$$\tilde{i}_u = \frac{1}{L} \times \begin{cases} -\bar{v}_{uv}(t-t_o) & \text{for } t_o < t \leq t_1 \\ -\bar{v}_{uv} \frac{T_0}{4} + (E_d - \bar{v}_{uv})(t-t_1) & \text{for } t_1 < t \leq t_2 \\ -\bar{v}_{uv}(t-t_3) & \text{for } t_2 < t \leq t_4 \\ -\bar{v}_{uv} \frac{T_0}{4} + (E_d - \bar{v}_{uv})(t-t_4) & \text{for } t_4 < t \leq t_5 \\ -\bar{v}_{uv}(t-t_6) & \text{for } t_5 < t \leq t_6 \end{cases} \quad (12)$$

Based on Eq. (12), the peak to peak value of current ripple, $\tilde{i}_{u,pp}$, is defined as

$$\tilde{i}_{u,pp} = \frac{\bar{v}_{uv} T_0}{L} \frac{1}{2} \quad (13)$$

Substituting Eqs. (2), (4), and (9) into Eq. (13), the following is obtained

$$\tilde{i}_{u,pp} = \frac{E_d}{2LF_s} k \sin \theta (1 - k \sin \theta) \quad (14)$$

Where F_s is the switching frequency of the PWM inverter. The average value of peak-to-peak current ripple over one fundamental output period, $\tilde{I}_{u,pp}$ is defined as

$$\tilde{I}_{u,pp} = \frac{1}{\pi} \int_0^\pi \tilde{i}_{u,pp} d\theta \quad (15)$$

Substituting Eq. (14) into Eq. (15) and performing the integration, the result is

$$\tilde{I}_{u,pp} = \frac{E_d k}{4LF_s \pi} (4 - k\pi) \quad (16)$$

Based on Eq. (14), the peak to peak output current ripple varies with switching frequency and angle θ . If the switching frequency is modulated, the peak to peak current ripple can be made constant or almost constant as in Eq. (16). How to vary the switching frequency will be discussed in the next section.

Variable Switching Frequency

It has been shown in the previous section that the peak to peak current ripple varies with the time, as a function of angle θ . Figure. 4(c) shows simulated results that shows the variation of peak to peak value of current ripple as a function of time. The current ripple is zero when the current is zero. In this case, is assumed that the DC voltage source is 200 Vdc, the load resistance is 15 ohm, the load inductance is 1 mH. The switching devices are switched at 3 kHz switching frequency.

If the switching frequency on Eq. (14) is modulated to maintain the peak-to-peak current ripple at constant value as given by Eq. (16), by equalizing Eq. (14) and Eq. (16), the switching frequency must vary according to the following equations:

$$\tilde{i}_{u,pp} = \tilde{I}_{u,pp} \quad (17)$$

$$\frac{E_d}{2Lf_s} k \sin \theta (1 - k \sin \theta) = \frac{E_d k}{4LF_s \pi} (4 - k\pi) \quad (18)$$

$$f_s = F_s \frac{2\pi}{4 - k\pi} \sin \theta (1 - k \sin \theta) \quad (19)$$

Where f_s is the new varying switching frequency. Although it varies over time, however the average value of the switching frequency over one fundamental period is still constant at F_s . As the average switching frequency is constant, it is expected that the switching losses are almost constant. Figure. 5 shows simulated result under variable switching frequency. It can be seen that the peak-to-peak current ripple is almost constant over one fundamental output period, as shown in Figure. 5(c).

The mean square value of the output current ripple over one carrier period is

$$\tilde{I}_u^2 = \frac{1}{T_s} \int_{t_o}^{t_o+T_s} \tilde{i}_u^2 dt \quad (20)$$

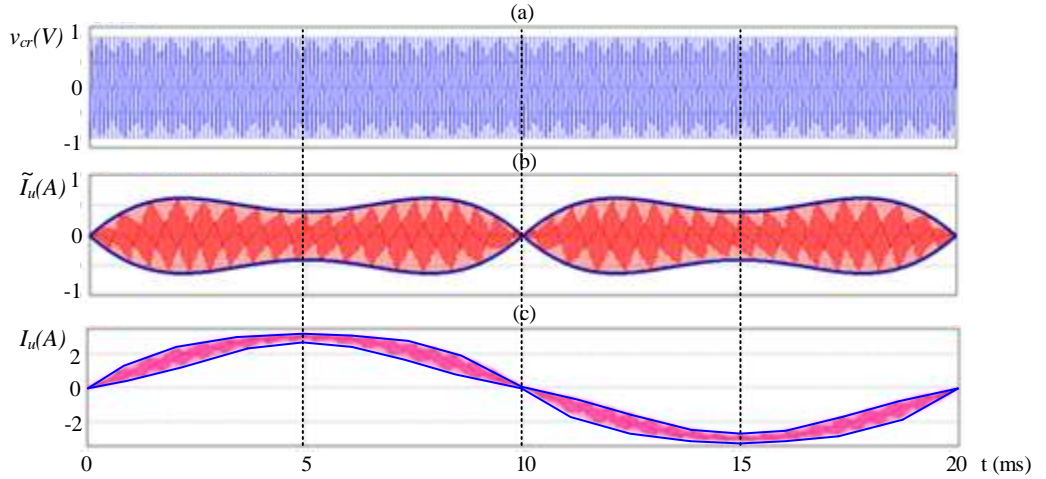


Figure. 4. Constant switching frequency operation. (a) Carrier waveform, (b) output current ripple, and (c) inverter output current.

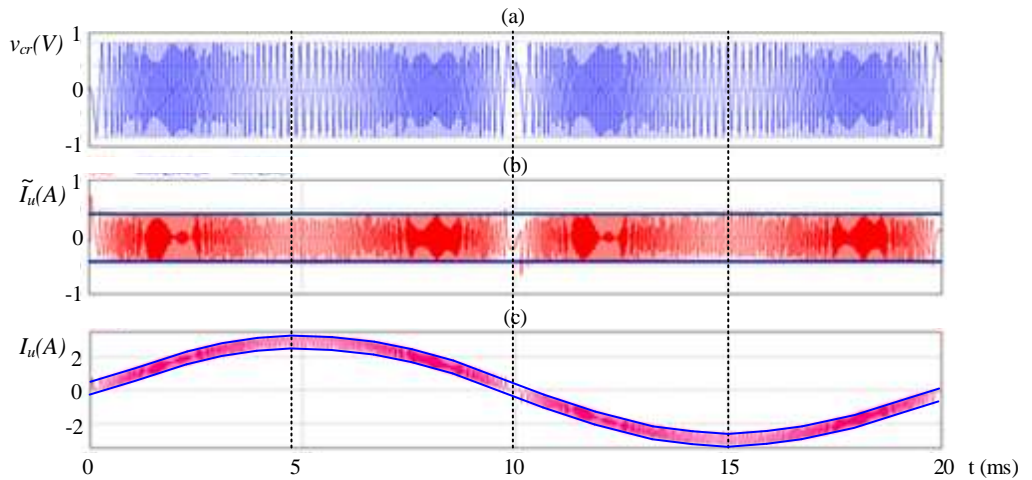


Figure. 5. Variable frequency operation. (a) Carrier waveform, (b) output current ripple, and (c) output current.

Substituting Eq. (12) into Eq. (20) and performing the integration, the following is obtained

$$\tilde{I}_u^2 = \left(\frac{E_d k}{L F_s} \right)^2 \frac{\sin^2 \theta (1 - k \sin \theta)^2}{48} \quad (21)$$

The rms value of output current ripple over one fundamental output period can be determined as

$$\tilde{I}_{u,rms} = \sqrt{\frac{1}{2\pi} \int_0^{2\pi} \tilde{I}_u^2 d\theta} \quad (22)$$

Under constant switching frequency, the result of Eq. (22) is

$$\tilde{I}_{u,rms} = \frac{E_d k}{L F_s} \left[\frac{1 - \frac{16}{3\pi} k + \frac{3}{4} k^2}{96} \right]^{1/2} \quad (23)$$

Under variable switching frequency, the rms current ripple is

$$\tilde{I}_{u,rms} = \frac{E_d k (4 - k\pi)}{L F_s 8\pi\sqrt{3}} \quad (24)$$

In the next section, experimental results will be shown to verify the effectiveness of the proposed method.

Experimental Results

In order to verify the proposed concept, a small single-phase PWM inverter was constructed. Power MOSFETS were used as the switching devices. The load resistance is 15 ohm and load inductance is 1 mH. No load emf is used during the experiments. During the experiments, the dc source voltage is maintained constant at 200 Vdc. The PWM controller is digitally implemented using FPGA. A low switching frequency of 3 kHz is used so that the current ripple can be easily measured.

Figures 6 and 7 show the measured current waveforms under constant and variable switching frequencies. It can be seen that the peak-to-peak current ripple can be maintained constant by the proposed variable frequency method in Figure.7, instead of varying peak-to-peak current ripple in the conventional constant switching frequency operation, as in Figure. 6.

Figure 8 shows the measured rms current ripples under constant and variable switching frequency. It can be seen that by using the proposed variable switching frequency, the rms value of the output current ripple is lower than under constant switching frequency. Losses of the proposed and conventional methods are measured during the experiments. Measured results (Figure. 9) shows that the losses under both techniques are almost equal. Thus, the current ripple has been successfully reduced without increasing the switching losses.

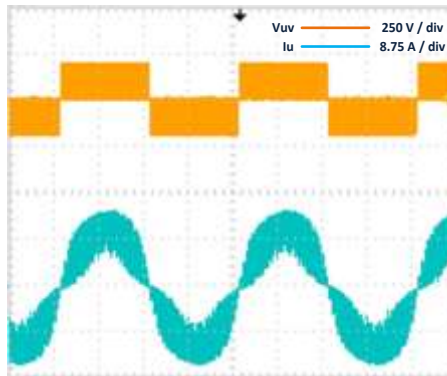


Figure 6. Measured output voltage (upper) and output current (lower) waveforms under constant switching frequency.

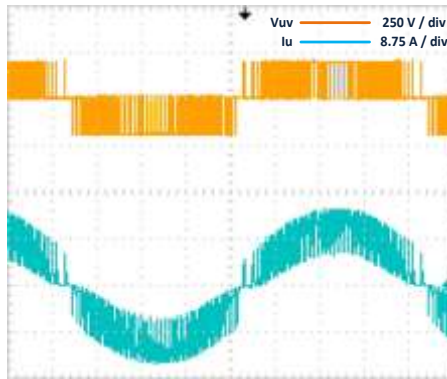


Figure 7. Measured output voltage (upper) and current (lower) under variable switching frequency.

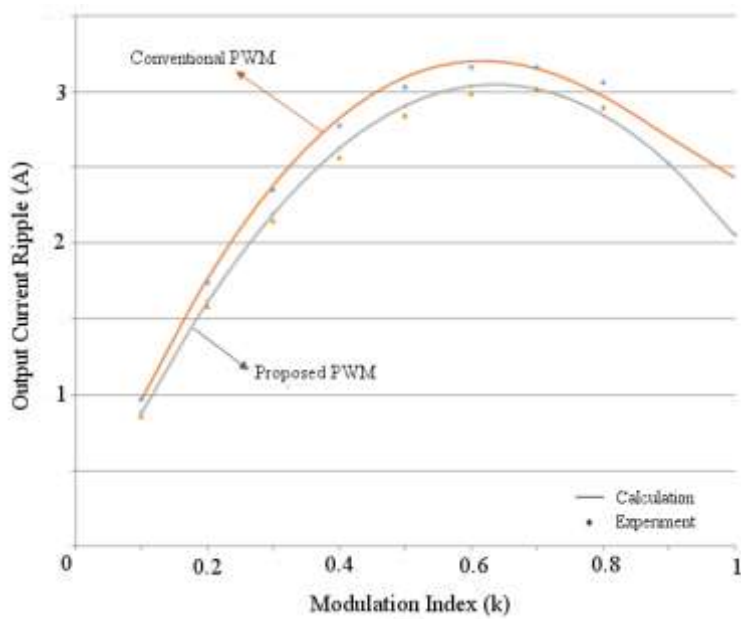


Figure 8. Measured rms values of output current ripple.

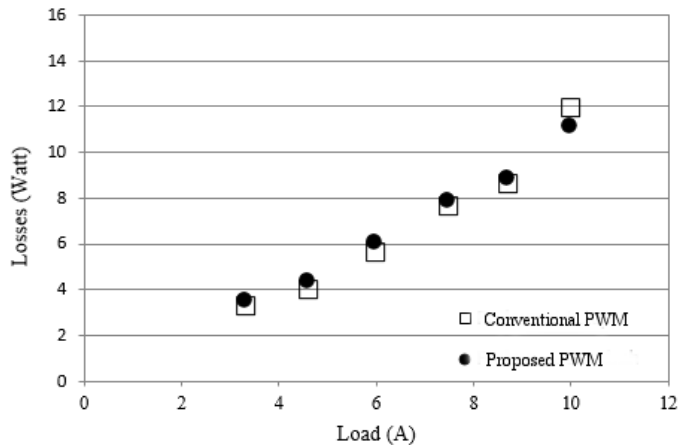


Figure 9. Measured losses of PWM inverter.

Conclusion

A new approach to enhance the performance of single-phase PWM inverter is proposed in this paper. The proposed variable switching frequency method is reducing the output current ripple without sacrificing switching losses. The expression for the required switching frequency is derived. Simulated and experimental results are included to show the effectiveness of the proposed method.

Acknowledgement

Authors would like to thank to Ministry of Research, Technology and Higher Education Indonesia for funding this research.

References

- [1]. S. B. Kjaer, J. K. Pedersen, and F. Blaabjerg, "A Review of Single-Phase Grid-Connected Inverters for Photovoltaic Modules," *IEEE Transactions on Industry Applications* Vol. 41 No. 5, Sep/Oct 2005.
- [2]. Y. Iwaji and S. Fukuda, "A Pulse Frequency Modulated PWM Inverter for Induction Motor Drives," *IEEE Trans. Power Electr.*, Vol. 7, No. 2, April 1992, pp. 404-410.
- [3]. M.J.Gutierrez, F.P. Hidalgo, F.V. Meriono, and J.R. Larrubia, "Pulse Width Modulation Technique with Harmonic Injection and Frequency Modulated Carrier: Formulation and Application to Induction Motor," *IET Power Appl.*, Vol. 1, No. 5, 2007, pp. 714-726.
- [4]. X. Mao, R. Ayyanar, and H.K. Krishnamurthy, "Optimal Variable Switching Frequency Scheme for Reducing Switching Losses in Single-Phase Inverters Based on Time-Domain Ripple Analysis," *IEEE Trans. Power Elect.* Vol. 24, No. 4, April 2009, pp. 991-1001.
- [5]. D. Jiang and F. Wang, "Variable Switching Frequency PWM for Three-Phase Converter Based on Current Ripple Prediction," *IEEE Trans. Power Electr.*, Vol. 28, No. 11, Nov. 2013, pp. 4951-4961.
- [6]. A.J. Sonawane, S.P. Gawande, S.G. Kadwane, and M.R. Ramteke, "Nearly Constant Switching Frequency Hysteresis-Based Predictive Control For Distributed Static Compensator Applications", *IET Power Electron.*, 2016, Vol. 9, Iss. 11, pp. 2174–2185.
- [7]. F. Wu, F. Feng, L. Luo, J. Duan, and L. Sun, "Sampling Period Online Adjusting-Based Hysteresis Current Control Without Band With Constant Switching Frequency", *IEEE Trans. Ind. Electr.*, Vol. 62, No. 1, Jan 2015, pp. 270 – 277.
- [8]. C.N. Ho, V.P. Cheung, H.S. Chung, "Constant-Frequency Hysteresis Current Control of Grid-Connected VSI Without Bandwidth Control", *IEEE Trans. Power Electr.*, Vol. 24, No. 11, Nov 2009, pp. 2484 – 2495.
- [9]. Dey, N.A. Azeez, K. Mathew, K.N. Gopakumar, and M.P. Kazmierkowski, "Hysteresis Current Controller For A General N-Level Inverter Fed Drive With Online Current Error Boundary Computation And Nearly Constant Switching Frequency", *IET Power Electron.*, 2013, Vol. 6, Iss. 8, pp. 1640–1649.
- [10]. Fereidouni, M.A.S. Masoum, and K.M. Smedley, "Supervisory Nearly Constant Frequency Hysteresis Current Control for Active Power Filter Applications in Stationary Reference Frame", *IEEE Power and Energy Technology Systems Journal*, Vol. 3, No. 1, March 2016, pp. 1 – 12.



Pekik Argo Dahono received the bachelor degree from the Department of Electrical Engineering, Institut Teknologi Bandung, Indonesia, in 1985, and the M.Eng. and D.Eng. degrees in engineering from the Department of Electrical and Electronic Engineering, Tokyo Institute of Technology, Tokyo, Japan, in 1992 and 1995, respectively.

Since 1986, he has been with the School of Electrical Engineering and Informatics, Institute of Technology Bandung, where he is currently an Associate Professor. He was a Japan Society for the Promotion of Science Research Fellow and Hitachi Post Doctoral Fellow at Tokyo Institute of Technology in 1997 and 1998, respectively. He was a Visiting Professor at the Science University of Tokyo and Tokyo Denki University in 2001 and 2004, respectively. He was also a Visiting Professor at the Institut National Polytechnique Toulouse (INPT), Toulouse, France, in 2008. His research interests include power electronics, electrical machines, and power quality.

Dr. Dahono is a senior member of IEEE and also registered as a Senior Professional Engineer in Indonesia. He was the recipient of Outstanding Engineering Achievement Awards from the Institution of Engineers Indonesia and the ASEAN Federation of Engineering Association, in 2005 and 2006, respectively.



Masramdhani Saputra was born in Batu, Indonesia, on March 28, 1991. He received B.Sc (cumlaude) and M.Sc degrees from Institute of Technology, Bandung, Indonesia, in 2013 and 2014, respectively. He was with Electrical Conversion Energy Laboratory, Institut Teknologi Bandung until 2014, as researcher. His current research interests control techniques for bidirectional power converters and new pulse width modulation techniques for single-phase PWM Converter. Now he is with Malang State Polytechnic, Malang, Indonesia, as a lecturer.



Arwindra Rizqiawan received the bachelor and master degrees in electrical engineering from the School of Electrical Engineering and Informatics, Institut Teknologi Bandung, Indonesia, in 2006 and 2008, respectively. He received the D.Eng. degree in electrical engineering from Shibaura Institute of Technology, Japan, in 2012, where he continued with post-doctoral program in 2013. Since 2014, he has been with School of Electrical Engineering and Informatics, Institut Teknologi Bandung, Indonesia. He is registered as a Professional Engineer in Indonesia. His research interests include power electronics, renewable energy, and distributed generation.